Geoderma 443 (2024) 116810

Contents lists available at ScienceDirect

Geoderma

journal homepage: www.elsevier.com/locate/geoderma

Decreasing carbon allocation belowground in alpine meadow soils by shrubification

Xiao Ming Mou [a,b], Fen-Can Li [a], Bin Jia [a], Jie Chen [a], Zhen-Huan Guan [a], Yu-Qiang Li [b], Georg Guggenberger [c], Yakov Kuzyakov [d,e], Lin Wang [a], Xiao Gang Li [a,*]

[a] College of Ecology, Lanzhou University, Lanzhou, 730000, China
[b] Northwest Institute of Eco-Environment and Resources, Naiman Desertification Research Station, Chinese Academy of Sciences, Lanzhou, Gansu 730000, China
[c] Leibniz University Hannover, Institute of Soil Science, Hannover, Germany
[d] Department of Soil Science of Temperate Ecosystems, Department of Agricultural Soil Science, University of Goettingen, 37077 Göttingen, Germany
[e] Peoples Friendship University of Russia (RUDN University), 117198 Moscow, Russia

ARTICLE INFO

Handling Editor: C. Rumpel

Keywords:
^{13}C pulse labelling
Photosynthate allocation belowground
phospholipid fatty acids (PLFAs)
Herbaceous plants
Shrub expansion

ABSTRACT

Distribution of shrubs expanding in grasslands – shrubification – is ongoing worldwide in grasslands and is common on the Qinghai–Tibetan Plateau (QTP). But the consequences of shrubification for plant carbon (C) input and fate in soil are unclear. We used ^{13}C pulse labelling in a meadow on the QTP to compare photosynthetic capacity and photosynthate distribution in shoots, roots, soil and microbial functional groups between herbaceous plants (herbs) and shrubby *Potentilla fruticosa*. During 3 h of labeling in $^{13}CO_2$ atmosphere, the ^{13}C amount assimilated by shrubs (0.81 g C/m^{-2}) was only 38 % of that by herbs. Over 8 days after labeling, ^{13}C amount respired jointly by roots and soil microorganisms under shrubs (0.049 g m^{-2}) was less than half of that under herbs. The mean residence time of ^{13}C for respiration jointly by roots and rhizosphere microorganisms was longer under shrubs (0.61 day) than under herbs (0.44 day). Within 22 days after labelling, ^{13}C amounts in roots, soil, and microorganisms were consistently smaller under shrubs than those under herbs. Consequently, shrub *P. fruticosa* had not only smaller photosynthetic potential, but also allocated less photosynthate belowground and slowed down C cycling in soil compared with herbs. The distribution of total ^{13}C in microbial functional groups indicated by PLFA analysis was similar between herbs and shrubs. Averaged over vegetation patch types, gram negative bacteria and AMF accounted for 22 % and 4 % of the total microbial PLFAs in the 0–20 cm, respectively, but these two functional groups took up 51 % and 23 % of the total ^{13}C absorbed by microorganisms, respectively. This indicates that gram negative bacteria and AMF are major consumers of rhizodeposits. Concluding, shrubification leads to smaller C allocation belowground and slows down C cycling in the soil.

1. Introduction

The Qinghai–Tibet Plateau is a huge organic carbon (C) reservoir, which is, however, extremely sensitive to climate and land use changes (Qiu, 2008). Strong changes in ecosystems in the past several decades include the expansion of shrubs in grasslands due to overgrazing and global warming, the process named “shrubification” (Brandt et al., 2013; Gao et al., 2016; Zhao et al., 2021). The effects of shrubification on soil organic C (SOC) storage have been rarely investigated, and how these effects depend on the plant carbon (C) input into soil is unclear.

The SOC storage is the balance between plant C input and microbial SOC mineralization. Photosynthate allocation belowground is the main pathway for plant C to enter the soil. It is estimated that around 33 % of the photoassimilates in global grasslands is allocated belowground (16 % incorporated into roots, 5 % as rhizodeposits, and 12 % is lost as root and microbial respiration) (Pausch and Kuzyakov, 2018). Rhizodeposits are important nutrient and energy sources for soil biota, and their utilization and transformation by microorganisms is a major process of SOC formation (Högberg and Read, 2006; Brüggemann et al., 2011; Kuzyakov and Razavi, 2019).

Photosynthate allocation belowground depends on plant species and soil physico-chemical properties (Mokany et al., 2006; Pausch and Kuzyakov, 2018). Shrubs and herbaceous plants (herbs) differ greatly in morphology, physiology and life cycle (Sun et al., 2016; Ochoa-Hueso

* Corresponding author.
E-mail address: lixiaogang@lzu.edu.cn (X. Gang Li).

https://doi.org/10.1016/j.geoderma.2024.116810
Received 23 March 2023; Received in revised form 15 January 2024; Accepted 31 January 2024
Available online 10 February 2024

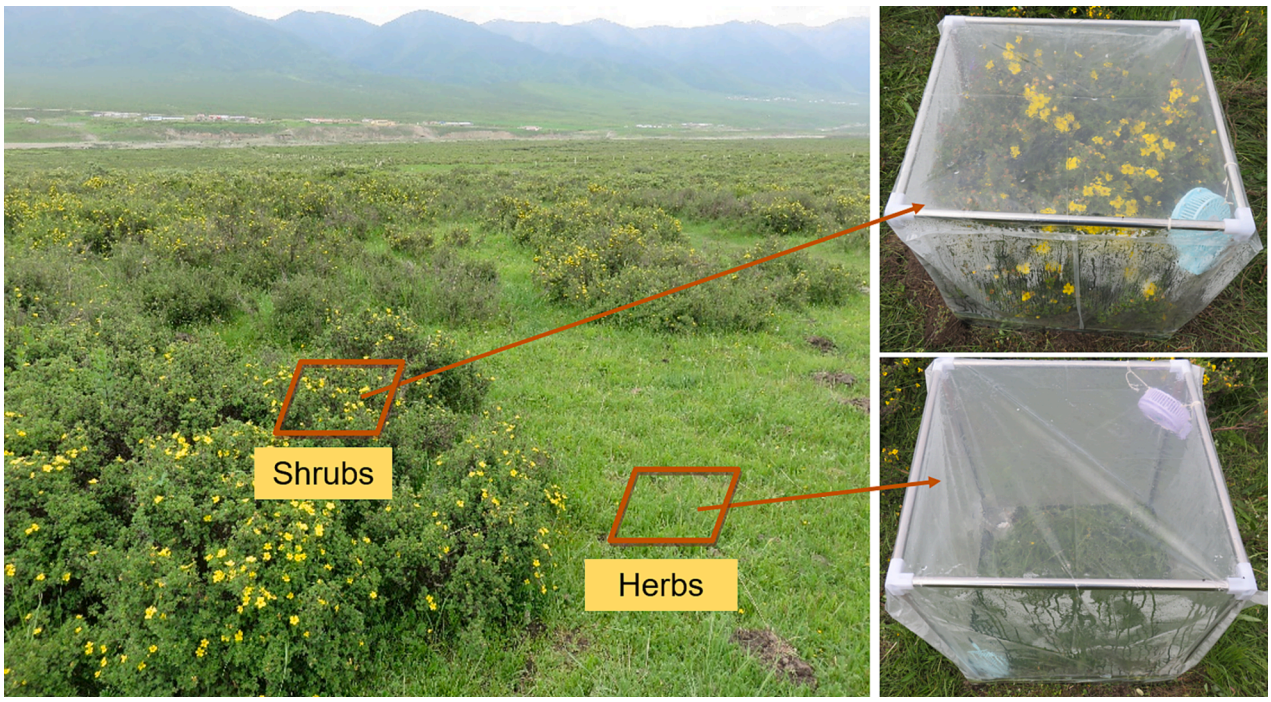

Fig. 1. *Potentilla fruticosa* meadow (102° 45′ E, 37° 12′ N, 2965 m above sea level) and the chambers for labeling in $^{13}CO_2$ atmosphere. Herbaceous species covered about 57 % of the meadow included *Polygonum viviparum*, *Kobresia capillifolia*, *Potentilla multifida* and *Poa crymophila*, while shrubby *P. fruticose* (45–55 cm height) occupied about 43 %. The dimensions of each labeling chamber were 50 cm wide × 50 cm long × 60 cm high (150 L in volume).

et al., 2017; Zhou et al., 2019). Therefore, shrubs and herbs should differ in their photosynthetic capacities and allocation patterns of photosynthate between aboveground and underground parts. In addition, varying quantity, and composition of rhizodeposits may further alter soil microbial community composition and thus influence SOC accumulation (Bragazza et al., 2015; Elias et al., 2017; Ochoa-Hueso et al., 2017). However, the responses of rhizodeposition and its distribution among soil microbial groups to shrub expansion in alpine meadows remain largely unknown. Identifying differences in the photosynthate allocation to soil and microorganisms between shrubby and herbaceous plants is crucial to assess shrubification effects on C and nutrient cycling and SOC storage.

The present study used ^{13}C pulse labeling combined with ^{13}C-PLFA profiling to compare photosynthate allocation belowground and ^{13}C incorporation into SOC and microorganisms as well as release as CO_2 between shrubby *Potentilla fruticosa* and herbaceous plants in alpine meadows on the Tibetan Plateau. *P. fruticosa* is widely distributed in grasslands of the Northern hemisphere. The *P. fruticosa* meadow represents the second most abundant species vegetation type after *Kobresia humilis* meadow on the Tibetan Plateau (Zhou and Wu, 2001). Warming experiments have shown that growth and abundance of *P. fruticosa* is increasing with temperature particularly in cold regions (Klein et al., 2007; Elmendorf et al., 2012). We hypothesized that shrubby *P. fruticosa* has a greater capacity to allocate photosynthate C belowground due to larger root biomass of *P. fruticosa*, compared with herbs.

2. Materials and methods

2.1. Site and experimental design

The research site was in Tianzhu Zang Autonomous County, Gansu Province, China, about 2 km from the Gansu Agricultural University Alpine Grassland experiment station (102° 45′ E, 37° 12′ N, and altitude 2965 m above sea level). The mean annual temperature and precipitation are –0.1 °C and 416 mm, respectively, with a growing season of 120 days (June–September). The $^{13}CO_2$ labeling experiment was conducted in a meadow with an area of about 10 ha.

The meadow was used for grazing yaks (*Bos grunniens*) and sheep (*Ovis aries*) in the winter season (November–June). The vegetation of the meadow was composed of shrub *P. fruticose* (a deciduous species, about 43 % in the cover and 45–55 cm in the height) and herbaceous species including *Polygonum viviparum*, *Kobresia capillifolia*, *Potentilla multifida* and *Poa crymophila*. The *P. fruticose* plants grew in compact patches (at least > 0.5 m in diameter) (Fig. 1). The shrubby *P. fruticose* and dominant herbaceous species have similar phenology. Growth begins in early June and maximum leaf area and flowering phase fall in early August. The soil is classified as Sub-alpine Meadow soil according to Chinese Soil Classification. The soil is developed from loess and has silty loam texture, with a pH value of 7.7 (Li et al., 2009), similar to a Cryrendoll (Wu and Tiessen, 2002).

2.2. ^{13}C pulse labeling

^{13}C pulse labeling was carried out on July 10, 2019 at 10:00 am, at clear sunny weather conditions. On the day before labeling, four replicated plots (each 4 m × 4 m) were randomly selected within a well vegetated area of 100 m × 100 m in the meadow. Within each plot, a representative *P. fruticosa* patch (45–55 cm high) was slightly trimmed into a square with an area of 0.25 m^{-2} (0.5 m × 0.5 m). All sporadically growing herbaceous species under shrubs were removed. A chamber consisting of a metal bracket covered by transparent polyethylene foil (0.5 m wide × 0.5 m long × 0.6 m high, 150 L in volume) was installed to cover the shrubby patch (Fig. 1). The metal bracket was fixed on a base that was made of an iron sheet (2 mm thick). The base was inserted into the soil to a depth of 0.2 m to cut off the roots between plants inside and outside the chamber. The inner surface of polyethylene foil was sprayed with anti-fog agent to reduce condensation of water evaporation. A representative patch of herbaceous plants (0.5 m × 0.5 m) about 2 m away from the confined *P. fruticosa* patch was delineated and another chamber was installed to cover the herbaceous patch in the same manner as for the shrub patch. As such, we labeled 4 pairs (replicates) of treatments (shrubs versus herbaceous plants).

Each chamber had been closed for 30 min to consume the existing atmospheric CO_2 inside before labeling. During the 30 min, CO_2 concentrations inside chambers were recorded using a CO_2 monitor (GXH-3010E, Huayun Instrument Company, Beijing, China). The CO_2 concentration stabilized at about 305 ppm for shrub chambers and 292 ppm for herbaceous chambers. 100 mL of 2 M H_2SO_4 (about 20 mL every 10 min) was then injected into a beaker within each chamber to produce $^{13}CO_2$. The beaker contained 6.5 g $Na_2^{13}CO_3$ (98 atom% ^{13}C enriched, Shanghai Research Institute of Chemical Industry, China), corresponding to 0.77 g ^{13}C. To facilitate a uniform distribution of $^{13}CO_2$ in the chamber, two 5 V fans were installed inside in each chamber to mix the air. The labeling process lasted for 3 h. Before labeling, two ice bags were placed in each chamber to limit the rise of air temperature during the labeling. Air temperatures inside shrub and herbaceous chambers increased by about 1–2 °C at the end of labeling, relative to the ambient temperature.

2.3. Measurement of $^{13}CO_2$ efflux from soil

Immediately after labeling, an opaque PVC chamber (0.07 m diameter, 0.25 m high) was installed on the soil surface (inserted into the soil to a depth of 0.05 m) to collect CO_2 within the labeled area, where all aboveground biomass was removed. A beaker containing 1 M NaOH solution was placed inside the PVC chamber to trap CO_2 respired from the soil. The beaker was replaced by a new one on days 1, 2, 3, 5 and 8 after labeling. The volume of NaOH solution used was 20 mL for each of the first three samplings and 30 mL for the last two samplings. Each time when NaOH solution was replaced, newly growing herbaceous plants were cut off the ground. The quantity of CO_2 trapped in the NaOH solution was measured by titrating the residual NaOH with 0.1 M HCl in the presence of excess $SrCl_2$ using phenolphthalein as an indicator. Concentrations of NaOH solutions that had absorbed carbon dioxide for all vegetation patches over the whole $^{13}CO_2$ efflux measurement course ranged from 0.78 M to 0.94 M. After centrifugation, the $SrCO_3$ sediments were dried at 65 °C and ground to powder for analysis of $\delta^{13}C$ signature.

2.4. Plant and soil sampling

Shoots, roots, and soils were sampled on days 0 (immediately after the labeling), 1, 3, 8, and 22. On days 0, 1, 3 and 8 after labeling, two ramets (leaves and stems) from *P. fruticosa* in each ^{13}C-labeled *P. fruticosa* patch were harvested to analyze the $\delta^{13}C$ signature. The herbaceous shoots were cut at the ground surface from two small circles (0.03 m diameter) in each ^{13}C-labeled herbaceous patch. Soils were sampled using an auger (0.03 m inner diameter) at 0–0.2 and 0.2–0.5 m depth from two points, respectively, in each labeled patch. The roots were carefully sorted from the soil. The soils or roots at the same depth within a patch were pooled to form a composite sample to analyze the $\delta^{13}C$ signature.

On day 22 after labeling, all shoots were harvested from the ground on each labeled shrub or herbaceous patch. A small portion of each composite shoot biomass was sampled for measuring the shoot $\delta^{13}C$ signature and the remaining was used for measuring shoot biomass. Except for the collection of soil and root samples with a 0.085 m inner diameter auger, all other procedures were consistent with the aforementioned methods. A small portion of each composite root biomass was used to measure the root $\delta^{13}C$ signature and the remaining was used for estimating root biomass.

Plant samples (shoots and roots) and (bulk) soil samples for analysis of the $\delta^{13}C$ signature were placed in a liquid N tank and a portable refrigerator (<4 °C), respectively, for storage in the field and during transportation to the lab.

In the lab, root samples (for measuring root $\delta^{13}C$ signature and for estimating root biomass) were washed off on a 0.15 mm screen and dead roots were carefully removed based on their internal color (Hafner et al., 2012). After freeze-drying (SJIA-10 N, Ningbo, China), shoot and root samples for measuring ^{13}C signatures were ground in a ball mill (GT200, Beijing, China). Shoot or root samples used to measure biomass were oven-dried to the constant weight at 65 °C. Each soil sample was split into two portions. One portion was freeze-dried to measure $\delta^{13}C$ signature of SOC, the other portion was stored at –60 °C to analyze microbial phospholipid fatty acid (PLFA) contents and ^{13}C incorporation into PLFA.

In unlabeled areas, at each sampling, four replicate samples of the above-ground shoots, roots or soils were also taken from either shrubby or herbaceous patches in the same way as in the labeled patches. These plant and soil samples were used as references for measuring the natural abundance of ^{13}C in plants and soil, respectively.

Soil temperature was measured using button-type temperature recorders (WatchDogB100, Spectrum Technologies, Aurora, IL, USA) in two shrubby and two herbaceous areas beside the labeled patches. The temperature recorders were placed at a depth of 0.1 m. The soil bulk density was determined using a cutting ring method. The soil water content was measured gravimetrically by drying samples at 105 °C at each sampling time.

2.5. Analyses of photosynthetic C distributions in plant parts, soil and released CO_2

The $\delta^{13}C$ signatures in soils, shoots, roots and $SrCO_3$ were determined using isotope ratio mass spectrometry coupled to an elemental analyzer (Delta V Advantage, Thermo Fisher Scientific, Waltham, USA) referenced to the international PDB standard. The SOC and C contents in shoots and roots were measured using an elemental analyzer (vario MACRO cube, Elementar, Hanau, Germany). Before determination of SOC contents and soil $\delta^{13}C$ signatures, freeze-dried soils (about 2 g each) were fumigated for four days to remove carbonates, in a desiccator containing 150 mL of concentrated HCl (37 %) (Ramnarine et al., 2011). After fumigation, soil was then left to stand for another four days in the desiccator to neutralize the soils, with the replacement of concentrated HCl solution by 150 mL 10 M NaOH solution. This procedure for removing carbonates was conducted separately for labeled and unlabeled (reference) soil samples. After carbonates were removed, soils were freeze-dried again and ground to powder by a ball mill.

The total ^{13}C assimilated by plants within each patch during labeling was the sum of ^{13}C amounts in shoots, roots, and soil in depths 0–0.2 m and 0.2–0.5 m measured immediately after labeling.

At each sampling time, the amount of ^{13}C derived from labeling in a C pool (shoots, roots, soil and CO_2 flux from soil) was calculated as:

$$^{13}C\ (g/m^{-2}) = {}^{13}C\%_{atom\ excess} \times \text{the size of the C pool } (g/m^{-2}).$$

where the sizes of shoot and root C were calculated by using shoot and root biomass measured on day 22 after labeling. The SOC stock was calculated using soil bulk density multiplied by depth and SOC content in each layer. The $^{13}C\%_{atom\ excess}$ was the difference in the percentage of ^{13}C atoms relative to the total C atoms ($^{13}C\%_{atom}$) between the labeled and natural abundance samples. The $^{13}C\%_{atom}$ was calculated from $\delta^{13}C$ that is the ^{13}C signature (‰) in a C pool relative to the international PDB standard with R_{PDB} of 0.011237.

To estimate the combined turnover rate (TR) of the rhizodeposits and plant assimilates released as CO_2, an exponential decay function (Hafner et al., 2012) was fitted to the rate of $^{13}CO_2$ efflux from the soil:

$$C_t = C_0 \times e^{-kt}$$

where C_t (mg $^{13}C\ m^{-2}$ soil day^{-1}) was the $^{13}CO_2$ efflux rate at time t (day) and C_0 was the initial rate of $^{13}CO_2$ efflux shortly after the labeling. k was the decay constant corresponding to the TR (day^{-1}). The combined mean residence time (MRT, day) of ^{13}C for respiration in rhizodeposits and roots was calculated as the reciprocal of the TR:

$$MRT = 1/TR$$

2.6. Analyses of photosynthetic C distributions in soil microbial groups

Phospholipid fatty acids (PLFAs) were extracted from field-moist soil (equivalent to 3 g of dry weight) according to the procedure described by Frostegård et al. (1993) and Kontro et al. (2006). Lipid fractions were separated by silicic acid columns (HF Bond Elut LRC-SI 500 mg, Varian, California, USA). Neutral lipids were eluted with chloroform, glycolipids with acetone and phospholipids with methanol. The solvent of the phospholipid fraction was evaporated under N_2 and samples were stored at –20 °C until fatty acids were saponified, methylated and extracted as methyl esters (Kontro et al., 2006). Methyl nonadecanoate fatty acid (19:0) was added prior to derivatization as an internal standard to quantify the concentrations of phospholipids. Individual fatty acid methyl esters (FAMEs) were identified and quantified using gas chromatography–mass spectrometry (Thermo Fisher Trace 1310, Waltham, USA) equipped with an HP-5 capillary column (30 m × 0.25 mm × 0.25 μm). The $\delta^{13}C$ values of FAMEs were determined by gas chromatography combustion isotope ratio mass spectrometry (GC-C-IRMS, Delta V Advantage, Thermo Fisher Scientific, Waltham, USA).

PLFAs were divided into five groups to indicate five respective microbial groups: (i) anteiso and iso PLFAs (i14:0, i15:0, a15:0, i16:0, a16:0, i17:0, a17:0 and 18:0 branched) for G^+ bacteria; (ii) monounsaturated and cyclic PLFAs (16:1ω7c, 18:1ω7c, 18:1ω9c, cy17:0 and cy19:0) for G^- bacteria; (iii) polyunsaturated PLFAs (18:2ω6,9) for saprophytic fungi; (iv) monounsaturated PLFA (16:1ω5c) for AMF, and (v) mid-chain branched PLFAs (10-me16:0 and 10-me 18:0) for actinomycetes (Smith et al., 2015; Zhu et al., 2017; Nowak et al., 2018; Zheng et al., 2021).

At each sampling, the ^{13}C existing in a PLFA was calculated as below:

$$^{13}C\ (g/m^{-2}) = {}^{13}C\%_{atom\ excess} \times \text{the size of PLFA pool } (g/m^{-2}) \times \text{mass fraction of C in a molecule of the PLFA}$$

The PLFA ($\delta^{13}C_{PLFA}$) was derived from a mass balance equation below (Denef et al., 2007):

$$\delta^{13}C_{PLFA} = [(n + 1) \times \delta^{13}C_{FAME} - \delta^{13}C_{MeOH}]/n$$

where n is the number of C atom of the PLFA molecule, $^{13}C_{FAME}$ is the measured $\delta^{13}C$ value of the FAME that was methylated from the PLFA, and $\delta^{13}C_{MeOH}$ is the measured value (–37 ‰) of methanol used for methylation. The number of C atom of a methanol molecule (equal to 1) was omitted.

The ^{13}C amount used by a group of microorganisms was the sum of ^{13}C contained in all PLFAs that were employed to indicate the microbial group.

2.7. Statistics

Differences in stocks of C present as plant shoots and roots and SOC (0–0.2, 0.2–0.5 m) between vegetation were compared using paired-*t* test at $p \leq 0.05$. Significant differences in all dynamically measured parameters (^{13}C partitioning in various plant and soil C pools, soil respiration, total PLFA, ^{13}C-PLFA and abundance of C-PLFA) between herbs and shrubs were identified also by using paired-*t* test at $p \leq 0.05$ within each sampling date. All data pools followed the normal distribution, with homoscedasticity. All statistical analyses were performed using SPSS 20.0 (IBM Corporation, Chicago, IL, USA).

3. Results

3.1. Soil temperature, water content and carbon pools of plant and soil

Daily soil temperature at 0.2 cm depth was by 3.9 °C lower under shrubs than under herbs during three weeks after labeling ($p < 0.05$)

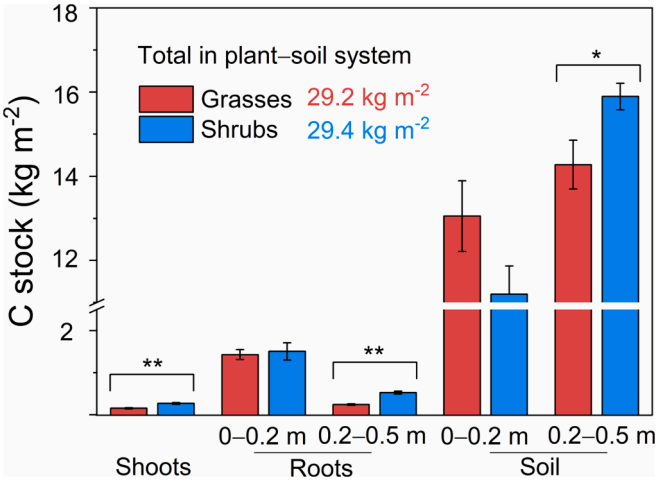

Fig. 2. Stocks of carbon (C) present as plant shoots and roots and soil organic C (0–0.2, 0.2–0.5 m) under herbs and shrubs (*Potentilla fruticosa*). Data are means ± 1 standard error (n = 4). Asterisks show differences between herbs and shrubs are significant at $p \leq 0.05$ (*), $p \leq 0.01$ (**).

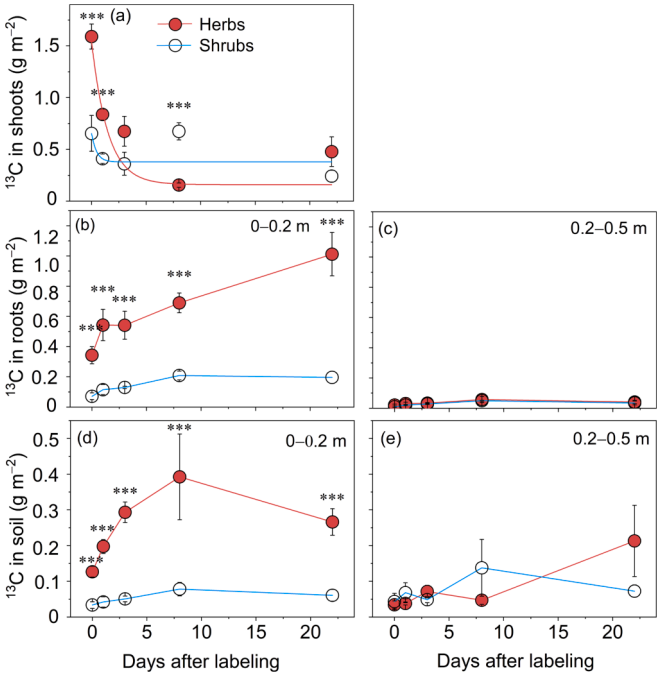

Fig. 3. Dynamics of ^{13}C amounts in shoots (a), roots (b, c) and in the 0–0.2 and 0.2–0.5 m soil depth (d, e) under herbs and shrubs (*Potentilla fruticosa*) after ^{13}C labeling. Bars are ± 1 standard errors (n = 4). Asterisks indicate significant differences in means between herbs and shrubs at $p \leq 0.001$ (***).

(Fig. S1a), while soil water content was similar between herbaceous and shrub patches ($p > 0.05$) (Fig. S1b). Soil bulk density in the 0–0.2 m was lower under shrubs (0.70 ± 0.03 g cm^{-3}) than under herbaceous plants (0.86 ± 0.05 g cm^{-3}) ($p < 0.05$) but in 0.2–0.5 cm was similar.

Aboveground biomass was 554 ± 49 g m^{-2} in *P. fruticosa* patches (405 g woody stems m^{-2} plus 150 g leaves m^{-2}), contrasting with 344 ± 32 g m^{-2} in herbaceous patches ($p < 0.01$). The shoot C stock under shrubs was 43 % higher than that under herbaceous species (Fig. 2). Root C and SOC stocks in the top 0.2 m were similar under herbaceous plants and shrubs but in the 0.2–0.5 m depth they were both larger under shrubs (Fig. 2).

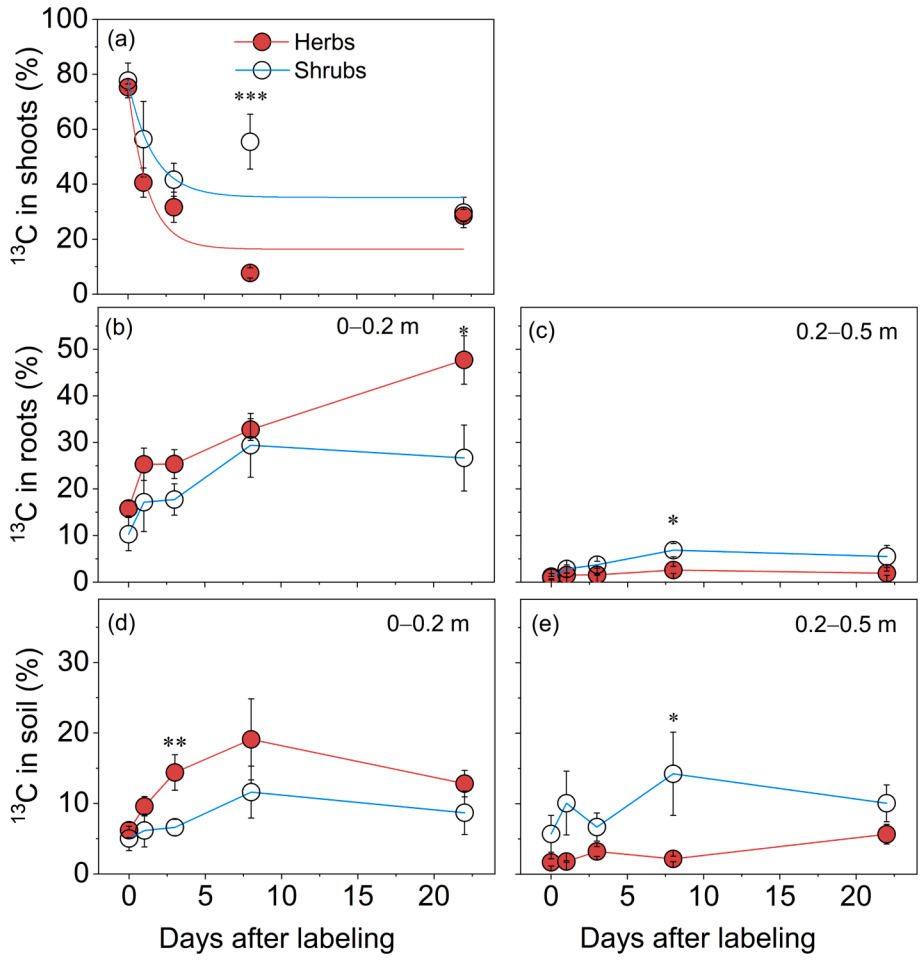

Fig. 4. Dynamics of ^{13}C allocation (% of total ^{13}C assimilated) among plant shoots (a), roots (b, c), and in the 0–0.2 and 0.2–0.5 m soil depth (d, e) under herbs and shrubs. Bars are ± 1 standard errors (n = 4). Asterisks indicate significant differences in means between herbs and shrubs at $p \leq 0.05$ (*), $p \leq 0.01$ (**) or $p \leq 0.001$ (***).

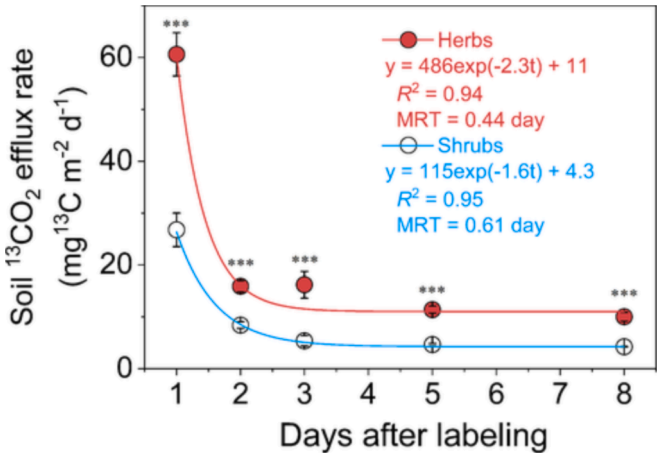

Fig. 5. Temporal courses of the $^{13}CO_2$ efflux rates from soil under herbs and shrubs. Bars are ± 1 standard errors (n = 4). Asterisks show significant differences in means between herbs and shrubs at $p \leq 0.001$ (***).

3.2. *^{13}C assimilation and distribution in plant parts, soil and CO_2 emission*

Immediately after labeling, ^{13}C amount recovered in shoots was smaller in shrubs than in herbs (Fig. 3a). ^{13}C amount in both roots and soil at 0–0.2 m depth was smaller under shrubs than under herbs, but it was similar at 0.2–0.5 m depth between the two types of vegetation (Fig. 3b, c, d, e). Adding ^{13}C in shoots, roots, and soil, 26 % and 68 % of the applied ^{13}C (0.77 g ^{13}C per chamber) were recovered in shrubs and herbs, respectively. Consequently, the ^{13}C assimilated by shrubs was only about one third of that by herbaceous plants.

The ^{13}C amount remaining in shoots in the first three days after labeling was smaller in shrubs than in herbs, but thereafter up to the day 22 it was generally similar (Fig. 3a). Immediately after labeling up to day 22, the ^{13}C amount in either roots or soil at the 0–0.2 m was smaller under shrubs than under herbs but at the 0.2–0.5 m depth was similar (Fig. 3b, c, d, e). On day 22 after labeling, summing up roots and soil in the entire 0.5 m profile, 0.365 ± 0.087 g ^{13}C m^{-2} remained under shrubs, less than one fourth of that under herbs (1.500 ± 0.292 g ^{13}C m^{-2}).

Within 22 days after labeling, the ^{13}C proportions allocated in shoots were generally greater for shrubs than for herbs (Fig. 4a). However, the ^{13}C proportions allocated to roots and soil in the top 0.2 m were generally smaller under shrubs than under herbs, but in the 0.2 to 0.5 m depth increment were generally greater under shrubs (Fig. 4b, c, d, e).

The $^{13}CO_2$ efflux rates from soil measured on days 1, 2, 3, 5 and 8 under shrubs were all smaller than those under herbs (Fig. 5). Over the entire 8 days after labeling, total ^{13}C respired under shrubs (0.049 ± 0.005 g m^{-2}) was less than half that under herbs (0.114 ± 0.009 g m^{-2}). The ^{13}C respired over the 8 days took up about 8.61 % and 6.94 % of total assimilated ^{13}C under shrubs and herbs, respectively. The mean residence time (MRT) of allocated ^{13}C that was used by roots and

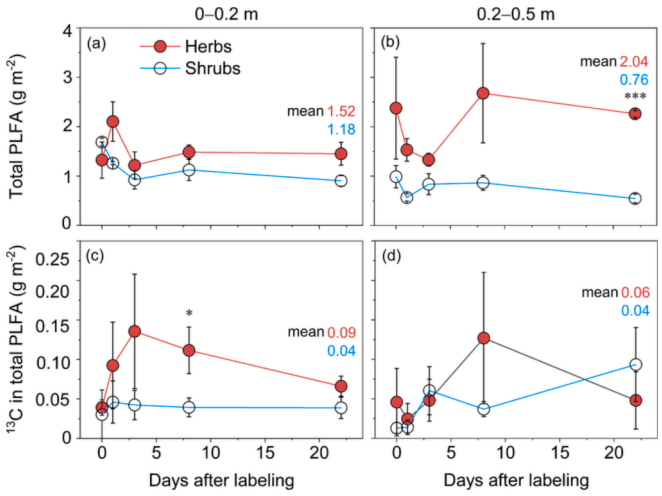

Fig. 6. Dynamics of total microbial PLFA content in soil (a, b) and ^{13}C incorporated into total PLFA (c, d) in the 0–0.2 and 0.2–0.5 m soil depth increments under herbs and shrubs. Bars are ± 1 standard errors (n = 4). Asterisks indicate significant differences in means between herbs and shrubs at $p \leq 0.05$ (*) or $p \leq 0.001$ (***).

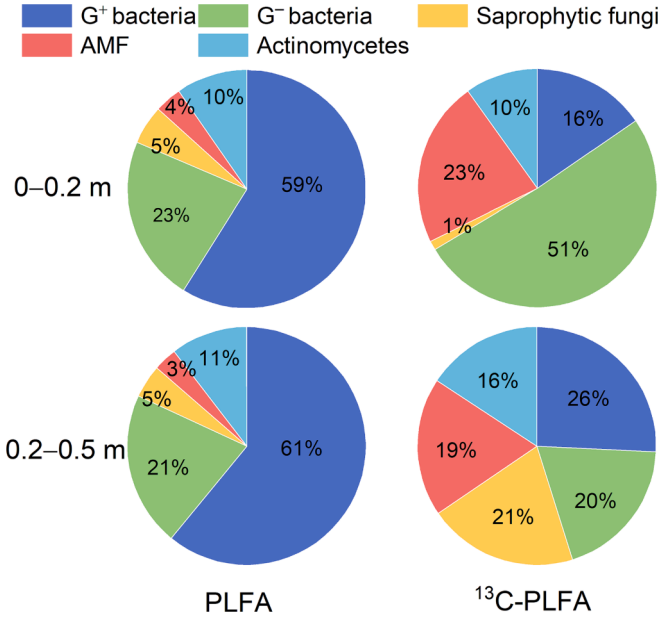

Fig. 7. Distribution of total PLFA (left) and ^{13}C incorporated into total PLFA (right) among five microbial groups (G^+ and G^- bacteria, saprophytic fungi, AMF and actinomycetes) at 0–0.2 and 0.2–0.5 m soil depth. Data were calculated across replicates of plots, vegetation types (shrubs and herbs) and sampling dates (days 0, 1, 3, 8 and 22 after ^{13}C labeling).

rhizosphere microorganisms was longer under shrubs than under herbs (Fig. 5).

3.3. Distribution of photoassimilates within soil microbial groups

Total PLFA contents over 22 days in the 0–0.2 and 0.2–0.5 m soil were generally similar under shrubs and herbs (Fig. 6a, b). The distributions of total PLFA representing five microbial groups (G^+ bacteria, G^- bacteria, saprophytic fungi, AMF and actinomycetes) were all generally similar between vegetation in the 0–0.2 and 0.2–0.5 m depth increments ($p > 0.05$) (Fig. S2). Across vegetation types and sampling dates, G^+ bacteria were the most abundant, followed by G^- bacteria and saprophytic fungi, and AMF and actinomycetes were the least, at both the 0–0.2 and 0.2–0.5 m soil depths (Fig. 7).

The ^{13}C in total PLFA in the top 0.2 m was lower under shrubs than under herbs only on the day 8 after labeling (Fig. 6c). At 0.2–0.5 m soil depth, the ^{13}C-PLFA contents over the 22 days were similar between shrubs and herbs (Fig. 6d). On most sampling dates, ^{13}C distributions in PLFA of various microbial groups were all generally similar between shrubs and herbs (Fig. S3). Across sampling dates and vegetation types, G^- bacteria took up half of the ^{13}C used by microorganisms, whereas the ^{13}C portion recovered from saprophytic fungi was negligible in the top 0.2 m (<1%) (Fig. 7). However, at 0.2–0.5 m soil depth, shares of PLFA ^{13}C by G^+ bacteria, G^- bacteria, saprophytic fungi, AMF and actinomycetes were similar (around 20 % for each microbial group).

4. Discussion

4.1. ^{13}Carbon assimilation

The ^{13}C labeling demonstrated that shrubby *P. fruticosa* has smaller capacity to capture CO_2 from the atmosphere than herbs. The smaller photosynthetic capacity of shrubs than herbaceous species is consistent with a previous study by Chen et al. (2022), who reported lower natural $\delta^{13}C$ values in leaves and roots of *P. fruticosa* compared with herbs in alpine meadows. A low photosynthetic efficiency in plants is usually associated with low (more negative) $\delta^{13}C$ values (Farquhar et al., 1989; Bai et al., 2012). The lower photosynthetic capacity for other shrubby species compared to herbs has been also reported by Winkler et al. (2020) on the Colorado Plateau. The smaller photosynthetic potential of shrub *P. fruticosa* could be firstly related to a smaller photosynthetic area than herbs: the leaf biomass of *P. fruticosa* (150 g m^{-2}) was smaller than half of aboveground biomass of herbs (344 g m^{-2}). Secondly, differences in anatomical and physiological features of mesophyll likely existed between *P. fruticosa* and herbaceous plants, lowering photosynthetic capacity of *P. fruticosa*. Leaves of herbaceous plants serve a stronger sink of CO_2 in the Calvin Cycle compared with shrub leaves, along with greater velocity of RuBP regeneration and photosynthetic flux density (Loik and Holl, 2001; Rindyastuti et al., 2021).

4.2. ^{13}Carbon allocation belowground

The shrub *P. fruticosa* has smaller capacity to allocate photosynthate C belowground than herbaceous plants. This is evidenced by the fact that photosynthate ^{13}C amounts in roots and soil as well as their proportions of the total assimilated ^{13}C were all lower under shrubs than under herbaceous plants within 22 days after labeling. The smaller capacity to allocate photosynthate C belowground under shrubs than under herbaceous species was contrasted with greater root biomass under shrubs. As such, our hypothesis that shrubby *P. fruticosa* has a greater capacity to sequestrate photosynthate C belowground than herbs in meadows must be rejected. Indeed, in annual or perennial herbs, the rhizodeposition can increase with the root biomass (Van der Krift et al., 2001; Van Hecke et al., 2005; Pausch et al., 2013). Despite that root biomass is greater in shrubby than in herbaceous areas in meadows (Chen et al., 2022), it may be largely comprised of thick roots but fine roots may be not abundant in *P. fruticosa*. Fine roots are thought to be more efficient in rhizodeposition (Kuzyakov and Razavi, 2019). As such, making a comparison between shrubs and herbs, a reckoning of rhizodeposition based on root biomass is not reliable. Our results implied that increased SOC storage by shrubification (He & Li, 2016; Chen et al., 2022) was not associated with rhizodeposition rather than was determined by other factors such as aboveground litter input, root turnover rate and SOC mineralization rate. In the present study, the SOC stock was similar between shrubby and herbaceous areas (Fig. 2), contrary to previous results at another location (He & Li, 2016; Chen et al., 2022). This may suggest that the effect of shrubs on SOC content is site-dependent, depending on grazing intensity and climatic factors.

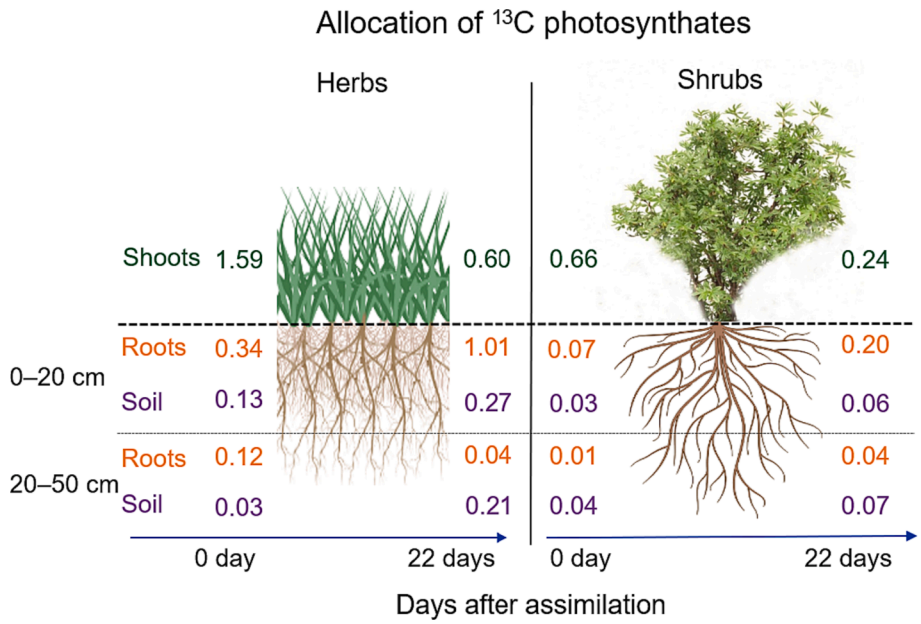

Fig. 8. ^{13}C amounts allocated into shoots, roots and soil on days of 0 and 22 after $^{13}CO_2$ assimilation by photosynthesis. Arrows at the bottom represent sampling time (days after labeling). The left- and right-hand panels show the data obtained for herbs and shrubs, respectively.

The lower photosynthate ^{13}C in roots and soil under shrubs than under herbs within 22 days after labeling was firstly ascribed to smaller photosynthetic capacity of shrub *P. fruticose*. Secondly, a smaller allocation rate of photosynthate from shoots to roots in shrubs than herbaceous plants was responsible for the lower accumulation of photosynthetic ^{13}C belowground. The smaller transfer rate of photosynthate belowground is evidenced by smaller ^{13}C amounts remaining in shoots in the first three days after labeling in shrubs than in herbaceous plants but thereafter was greater in shrubs (Fig. 3a). Despite that ^{13}C assimilated by shrubs was smaller, the proportion of photosynthate ^{13}C distributed in shoots was always higher in shrubs than in herbaceous plants during the 22 days after labeling (Fig. 4a).

In the 0.2–0.5 m depth, the portions of photosynthate ^{13}C in roots and soil were generally higher under shrubs (Fig. 4c, e). This is because *P. fruticose* is rooted deeper than herbs, thus delivering more photosynthate ^{13}C to deep soil. These findings may suggest that variations in root distribution caused by shrubification have a significant impact on the spatial distribution of SOC in the profile.

4.3. *^{13}Carbon respiration by roots and microorganisms*

We found that recently assimilated ^{13}C was respired slower from roots and soil and the MRT of belowground ^{13}C was longer under shrubs than under grasses. This indicates slower C cycling under shrubs. Smaller $^{13}CO_2$ flux from roots and soil under shrubs relative to herbs (Fig. 5) was firstly ascribed to smaller shrub capacity to allocate photosynthates into roots and soil. Secondly, soil temperature was 3.9 °C lower under shrubs than under herbs, lowering root and microbial activity. Finally, the lower CO_2 efflux from roots and soil under shrubs possibly reflected different chemical nature of belowground C between shrubs and herbs. Slow growing woody plants tend to accumulate more secondary metabolites in their tissues, with input of recalcitrant components to soils compared with fast growing herbs (Kögel-Knabner, 2002; Liao and Boutton, 2008). Root respiration is positively correlated with root decomposability and specific root length density but negatively with root diameter (Roumet et al., 2016).

4.4. *Microbial use of photosynthate*

The unchanged soil microbial community composition between shrubs and herbs, as revealed by PLFA profiling, was unexpected. The similar SOC content as well as similar other soil properties (e.g., pH, clay content) between areas under shrubs and herbs resulted in similar PLFAs content and microbial community composition and thus similar photosynthate C allocation in various microbial functional groups (Fierer and Jackson, 2006; Chen et al., 2014; Hu et al., 2014; Bragazza et al., 2015). Carey et al. (2015) also observed that soil microbial community structure is unaltered after shrub expansion in semi-arid Mediterranean-type grassland. Anyway, the effect of shrub expansion on soil microbial community composition in Tibetan grasslands needs further investigation.

Across shrubby and herbaceous vegetation patch types, microbial groups differed in their ability to use rhizodeposits. This was evidenced by the fact that in the top 0.2 m, across vegetation and sampling dates, G^+ and G^- bacteria groups accounted for 59 % and 23 % of total PLFA, respectively; but shared 16 % and 51 % of total ^{13}C in PLFA, respectively (Fig. 7). This indicates that G^- bacteria had much greater ability to use recent rhizodeposits than G^+ bacteria. The more efficient use of recent rhizodeposits by G^- bacteria than by G^+ bacteria has been also reported by De Deyn et al. (2011) in North West England grassland, Fuchslueger et al. (2014) in grasslands of the Austrian Central Alps, and Chaudhary and Dick (2016) in Switchgrass in greenhouse. G^- bacteria grow fast and thus are particularly important for C flow from roots through rhizosphere to stable SOC (Jin and Evans, 2010; Tavi et al., 2013; Tian et al., 2013; Ling et al., 2022). AMF in the top 0.2 m took up about 3–5 % of the total microbial PLFA, but shared 22 % of total ^{13}C-PLFA (Fig. 7). This indicates fast transfer of photosynthates to AMF symbionts. Saprophytic fungi used rhizodeposits at a very low level in the topsoil; however, in the 0.2–0.5 m depth, saprophytic fungi took up 5 % of the total microbial PLFA but shared 21 % of the total ^{13}C-PLFA. The difference of saprophytic fungi to use rhizodeposits in topsoil and subsoil was possibly associated with C limitation in the lower compared with the topsoil. Under C limitation in the lower depth, saprophytic fungi might have turned to preferentially acquiring rhizodeposited C.

5. Conclusions and ecological implications

^{13}Carbon labeling under real field conditions demonstrated that shrubs have smaller photosynthetic capacity, slower photosynthate transfer from shoots to roots and thus, release less rhizodeposits than

herbs in soil of alpine meadows (Fig. 8). Recently assimilated C was also respired slower from roots and soil under shrubs than under herbs. Shrubs, however, can deliver photosynthetic products deeper in the soil than herbs, due to greater rooting depth. This study suggests that making the comparison between shrubs and herbs, a reckoning of rhizodeposition by using root biomass is not reliable. Gram negative bacteria and AMF are major consumers of rhizodeposits in grasslands. Overall, shrubification reduces rhizodeposition and slows down C cycling in soil of alpine meadows. These results are crucial for understanding and predicting the consequences of plant community changes for C cycling in shrubification.

CRediT authorship contribution statement

Xiao Ming Mou: Methodology, Investigation, Formal analysis, Data curation, Writing – original draft, Writing – review & editing. **Fen-Can Li:** Investigation. **Bin Jia:** Methodology, Investigation, Formal analysis. **Jie Chen:** Investigation. **Zhen-Huan Guan:** Investigation. **Yu-Qiang Li:** Review & editing. **Georg Guggenberger:** Review & editing. **Yakov Kuzyakov:** Review & editing. **Lin Wang:** Investigation. **Xiao Gang Li:** Conceptualization, Methodology, Project administration, Supervision, Writing – original draft, Writing – review & editing.

Declaration of competing interest

The authors declare that they have no known competing financial interests or personal relationships that could have appeared to influence the work reported in this paper.

Data availability

Data will be made available on request.

Acknowledgments

This work was financed by the China Natural Science Foundation Program (Grant No. 42007078) and Youth Science and Technology Fund Program of Gansu Province (Grant No. 22JR5RA083). YK thanks the RUDN University Strategic Academic Leadership Program.

Appendix A. Supplementary data

Supplementary data to this article can be found online at https://doi.org/10.1016/j.geoderma.2024.116810.

References

Bai, E., Boutton, T.W., Liu, F., Wu, X.B., Hallmark, C.T., Archer, S.R., 2012. Spatial variation of soil $\delta^{13}C$ and its relation to carbon input and soil texture in a subtropical lowland woodland. Soil. Biol. Biochem. 44, 102–112.

Bragazza, L., Bardgett, R.D., Mitchell, E.A., Buttler, A., 2015. Linking soil microbial communities to vascular plant abundance along a climate gradient. New Phytol. 205, 1175–1182.

Brandt, J.S., Haynes, M.A., Kuemmerle, T., Waller, D.M., Radeloff, V.C., 2013. Regime shift on the roof of the world: Alpine meadows converting to shrublands in the southern Himalayas. Biol. Conserv. 158, 116–127.

Brüggemann, N., Gessler, A., Kayler, Z., Keel, S.G., Badeck, F., Barthel, M., Boeckx, P., Buchmann, N., Brugnoli, E., Esperschütz, J., Gavrichkova, O., Ghashghaie, J., Gomez-Casanovas, N., Keitel, C., Knohl, A., Kuptz, D., Palacio, S., Salmon, Y., Uchida, Y., Bahn, M., 2011. Carbon allocation and carbon isotope fluxes in the plant-soil-atmosphere continuum: a review. Biogeosciences 8, 3457–3489.

Carey, C.J., Beman, J.M., Eviner, V.T., Malmstrom, C.M., Hart, S.C., 2015. Soil microbial community structure is unaltered by plant invasion, vegetation clipping, and nitrogen fertilization in experimental semi-arid grasslands. Front. Microbiol. 6, 466.

Chaudhary, D.R., Dick, R.P., 2016. Identification of metabolically active rhizosphere microorganisms by stable isotopic probing of PLFA in switchgrass. Commun. Soil Sci. Plan. 47, 2433–2444.

Chen, J., Cui, H.Y., Jia, B., Gang, S., Li, Y., Li, F.C., Mou, X.M., Li, X.G., 2022. Soil sampling depth matters in assessing the impact of shrubification on soil organic carbon storage in grazed alpine meadows. Geoderma 426, 116119.

Chen, D., Mi, J., Chu, P., Cheng, J., Zhang, L., Pan, Q., Xie, Y., Bai, Y., 2014. Patterns and drivers of soil microbial communities along a precipitation gradient on the Mongolian Plateau. Landscape Ecol. 30, 1669–1682.

De Deyn, G., Quirk, H., Oakley, S., Ostle, N., Bardgett, R., 2011. Rapid transfer of photosynthetic carbon through the plant–soil system in differently managed species-rich grasslands. Biogeosciences 8, 1131–1139.

Denef, K., Bubenheim, H., Lenhart, K., Vermeulen, J., Van Cleemput, O., Boeckx, P., Muller, C., 2007. Community shifts and carbon translocation within metabolically-active rhizosphere microorganisms in grasslands under elevated CO_2. Biogeosciences 4, 769–779.

Elias, D.M.O., Rowe, R.L., Pereira, M.G., Stott, A.W., Barnes, C.J., Bending, G.D., McNamara, N.P., 2017. Functional differences in the microbial processing of recent assimilates under two contrasting perennial bioenergy plantations. Soil. Biol. Biochem. 114, 248–262.

Elmendorf, S.C., Henry, G.H.R., Hollister, R.D., Björk, R.G., Bjorkman, A.D., Callaghan, T.V., Collier, L.S., Cooper, E.J., Cornelissen, J.H.C., Day, T.A., Fosaa, A. M., Gould, W.A., Grétarsdóttir, J., Harte, J., Hermanutz, L., Hik, D.S., Hofgaard, A., Jarrad, F., Jónsdóttir, I.S., Keuper, F., Klanderud, K., Klein, J.A., Koh, S., Kudo, G., Lang, S.I., Loewen, V., May, J.L., Mercado, J., Michelsen, A., Molau, U., Myers-Smith, I.H., Oberbauer, S.F., Pieper, S., Post, E., Rixen, C., Robinson, C.H., Schmidt, N.M., Shaver, G.R., Stenström, A., Tolvanen, A., Totland, Ø., Troxler, T., Wahren, C.-H., Webber, P.J., Welker, J.M., Wookey, P.A., 2012. Global assessment of experimental climate warming on tundra vegetation: heterogeneity over space and time. Ecol. Lett. 15, 164–175.

Farquhar, G.D., Ehleringer, J.R., Hubick, K.T., 1989. Carbon isotope discrimination and photosynthesis. Annu. Rev. Plant Biol. 40, 503–537.

Fierer, N., Jackson, R.B., 2006. The diversity and biogeography of soil bacterial communities. P. Nati. Acad. Sci. USA 103, 626–631.

Frostegård, Å., Bååth, E., Tunlio, A., 1993. Shifts in the structure of soil microbial communities in limed forests as revealed by phospholipid fatty acid analysis. Soil. Biol. Biochem. 25, 723–730.

Fuchslueger, L., Bahn, M., Fritz, K., Hasibeder, R., Richter, A., 2014. Experimental drought reduces the transfer of recently fixed plant carbon to soil microbes and alters the bacterial community composition in a mountain meadow. New Phytol. 201, 916–927.

Gao, Q., Guo, Y., Xu, H., Ganjurjav, H., Li, Y., Wan, Y., Qin, X., Ma, X., Liu, S., 2016. Climate change and its impacts on vegetation distribution and net primary productivity of the alpine ecosystem in the Qinghai-Tibetan Plateau. Sci Total Environ. 554, 34–41.

Hafner, S., Unteregelsbacher, S., Seeber, E., Lena, B., Xu, X., Li, X., Kuzyakov, Y., 2012. Effect of grazing on carbon stocks and assimilate partitioning in a Tibetan montane pasture revealed by $^{13}CO_2$ pulse labeling. Glob. Change Biol. 18, 528–538.

He, J.L., Li, X.G., 2016. *Potentilla fruticosa* has a greater capacity to translocate phosphorus from the lower to upper soils than herbaceous grasses in an alpine meadow. Agr. Ecosyst. Environ. 228, 19–29.

Högberg, P., Read, D.J., 2006. Towards a more plant physiological perspective on soil ecology. Trends in Ecol. Evol. 21, 548–554.

Hu, Y., Xiang, D., Veresoglou, S.D., Chen, F., Chen, Y., Hao, Z., Zhang, X., Chen, B., 2014. Soil organic carbon and soil structure are driving microbial abundance and community composition across the arid and semi-arid grasslands in northern China. Soil. Biol. Biochem. 77, 51–57.

Jin, V.L., Evans, R.D., 2010. Microbial ^{13}C utilization patterns via stable isotope probing of phospholipid biomarkers in Mojave Desert soils exposed to ambient and elevated atmospheric CO_2. Glob. Change Biol. 16, 2334–2344.

Klein, J.A., Harte, J., Zhao, X.Q., 2007. Experimental warming, not grazing, decreases rangeland quality on the Tibetan Plateau. Ecol Appl. 17, 541–557.

Kögel-Knabner, I., 2002. The macromolecular organic composition of plant and microbial residues as inputs to soil organic matter. Soil. Biol. Biochem. 34, 139–162.

Kontro, M., Korhonen, L., Vartiainen, T., Pellikka, P., Martikainen, P.J., 2006. Selected ion monitoring in quantitative gas-liquid chromatographic-mass spectrometric detection of fatty acid methyl ester from environmental samples. J. Chromatogr. B 831, 281–287.

Kuzyakov, Y., Razavi, B.S., 2019. Rhizosphere size and shape: Temporal dynamics and spatial stationarity. Soil. Biol. Biochem. 135, 343–360.

Li, X.G., Zhang, M.L., Li, Z.T., Shi, X.M., Ma, Q., Long, R.J., 2009. Dynamics of soil properties and organic carbon pool in topsoil of zokor-made mounds at an alpine site of the Qinghai-Tibetan Plateau. Biol Fert. Soils 45, 865–872.

Liao, J.D., Boutton, T.W., 2008. Soil microbial biomass response to woody plant invasion of grassland. Soil. Biol. Biochem. 40, 1207–1216.

Ling, N., Wang, T., Kuzyakov, Y., 2022. Rhizosphere bacteriome structure and functions. Nat. Commun. 13, 836.

Loik, M.E., Holl, K.D., 2001. Photosynthetic responses of tree seedlings in grass and under shrubs in early-successional tropical old fields, Costa Rica. Oecologia 127, 40–50.

Mokany, K., Raison, R.J., Prokushkin, A.S., 2006. Critical analysis of root: shoot ratios in terrestrial biomes. Glob. Change Biol. 12, 84–96.

Nowak, K.M., Telscher, M., Seidel, E., Miltner, A., 2018. Unraveling microbial turnover and non-extractable residues of bromoxynil in soil microcosms with ^{13}C-isotope probing. Environ. Pollut. 242, 769–777.

Ochoa-Hueso, R., Hughes, J., Delgado-Baquerizo, M., Drake, J.E., Tjoelker, M.G., Pineiro, J., Power, S.A., 2017. Rhizosphere-driven increase in nitrogen and phosphorus availability under elevated atmospheric CO_2 in a mature Eucalyptus woodland. Plant Soil 416, 283–295.

Pausch, J., Kuzyakov, Y., 2018. Carbon input by roots into the soil: quantification of rhizodeposition from root to ecosystem scale. Glob. Change Biol. 24, 1–12.

Pausch, J., Tian, J., Riederer, M., Kuzyakov, Y., 2013. Estimation of rhizodeposition at field scale: Upscaling of a ^{14}C labeling study. Plant Soil 364, 273–285.
Qiu, J., 2008. China: the third pole. Nature 454, 393–396.
Ramnarine, R., Voroney, R.P., Wagner-Riddle, C., Dunfield, K.E., 2011. Carbonate removal by acid fumigation for measuring the $\delta^{13}C$ of soil organic carbon. Can. J. Soil Sci. 91, 247–250.
Rindyastuti, R., Hapsari, L., Byun, C., 2021. Comparison of ecophysiological and leaf anatomical traits of native and invasive plant species. J. Ecol. Environ. 45, 1–16.
Roumet, C., Birouste, M., Picon-Cochard, C., Ghestem, M., Osman, N., Vrignon-Brenas, S., Cao, K.F., Stokes, A., 2016. Root structure–function relationships in 74 species: evidence of a root economics spectrum related to carbon economy. New Phytol. 210, 815–826.
Smith, A.P., Marín-Spiotta, E., Balser, T., 2015. Successional and seasonal variations in soil and litter microbial community structure and function during tropical postagricultural forest regeneration: a multiyear study. Glob. Change Biol. 21, 3532–3547.
Sun, K., McCormack, M.L., Li, L., Ma, Z., Guo, D., 2016. Fast-cycling unit of root turnover in perennial herbaceous plants in a cold temperate ecosystem. Sci. Rep. 6, 19698.
Tavi, N.M., Martikainen, P.J., Lokko, K., Kontro, M., Wild, B., Richter, A., Biasi, C., 2013. Linking microbial community structure and allocation of plant-derived carbon in an organic agricultural soil using CO_2 pulse-chase labelling combined with ^{13}C-PLFA profiling. Soil. Biol. Biochem. 58, 207–215.
Tian, J., Dippold, M., Pausch, J., Blagodatskaya, E., Fan, M., Li, X., Kuzyakov, Y., 2013. Microbial response to rhizodeposition depending on water regimes in paddy soils. Soil. Biol. Biochem. 65, 195–203.
Van der Krift, T.A., Kuikman, P.J., Möller, F., Berendse, F., 2001. Plant species and nutritional-mediated control over rhizodeposition and root decomposition. Plant Soil 228, 191–200.
Van Hecke, M.M., Treonis, A.M., Kaufman, J.R., 2005. How does the fungal endophyte Neotyphodium coenophialum affect tall fescue (Festuca arundinacea) rhizodeposition and soil microorganisms? Plant Soil 275, 101–109.
Winkler, D.E., Belnap, J., Duniway, M.C., Hoover, D., Reed, S.C., Yokum, H., Gill, R., 2020. Seasonal and individual event-responsiveness are key determinants of carbon exchange across plant functional types. Oecologia 193, 811–825.
Wu, R., Tiessen, H., 2002. Effect of land use on soil degradation in alpine grassland soil, China. Soil Sci Soc Am J 66, 1648–1655.
Zhao, D., Zhu, Y., Wu, S., Zheng, D., 2021. Projection of vegetation distribution to 1.5 °C and 2 °C of global warming on the Tibetan Plateau. Global Planet. Change 202, 103525.
Zheng, T., Miltner, A., Liang, C., Nowak, K.M., Kästner, M., 2021. Turnover of gram-negative bacterial biomass-derived carbon through the microbial food web of an agricultural soil. Soil. Biol. Biochem. 152, 108070.
Zhou, L., Shen, H., Xu, Y., Li, H., Chen, L., Wang, Y., Zhang, P., Zhao, X., Liu, T., Hu, H., Fang, J., 2019. Soil organic carbon components in inner Mongolian shrub encroached grasslands. Plant Soil 442, 199–213.
Zhou, X.M., Wu, Z.L., 2001. Chapter 2 Flora traits and distribution of Kobresia meadow. In: Zhou, X.M. (Ed.), China *Kobresia* Meadows, Beijing, pp. 24–38.
Zhu, Z., Ge, T., Hu, Y., Zhou, P., Wang, T., Shibistova, O., Guggenberger, G., Su, Y., Wu, J., 2017. Fate of rice shoot and root residues, rhizodeposits, and microbial assimilated carbon in paddy soil-part 2: turnover and microbial utilization. Plant Soil 416, 243–257.